Genotype-specific responses to drought stress in Siberian wildrye (Elymus sibiricus): Insights from comparative physiological and transcriptomic analyses

Yongping An
Sichuan Zoige Alpine Wetland Ecosystem National Observation and Research Station, Southwest Minzu University

Qian Wang
Guizhou Academy of Agricultural Sciences

Yannong Cui
Northwest A&F University

Xin Liu
Huazhong Agricultural University

Ping Wang
Sichuan Zoige Alpine Wetland Ecosystem National Observation and Research Station, Southwest Minzu University

Yue Zhou
Sichuan Zoige Alpine Wetland Ecosystem National Observation and Research Station, Southwest Minzu University

Peng Kang
North Minzu University

Youjun Chen
Sichuan Zoige Alpine Wetland Ecosystem National Observation and Research Station, Southwest Minzu University

Zhiwei Wang
Guizhou Academy of Agricultural Sciences

Qingping Zhou
Sichuan Zoige Alpine Wetland Ecosystem National Observation and Research Station, Southwest Minzu University

Pei Wang
wangpei@swun.edu.cn

Sichuan Zoige Alpine Wetland Ecosystem National Observation and Research Station, Southwest Minzu University

---

Article

Keywords: Siberian wildrye, osmotic resistance, differentially expressed genes (DEGs), stress tolerance, ROS, ABA, cuticular wax

Posted Date: April 22nd, 2024

DOI: https://doi.org/10.21203/rs.3.rs-4251832/v1

Additional Declarations: No competing interests reported.

Version of Record: A version of this preprint was published at Scientific Reports on September 10th, 2024. See the published version at https://doi.org/10.1038/s41598-024-71847-9.

Genotype-specific responses to drought stress in Siberian wildrye (*Elymus sibiricus*): Insights from comparative physiological and transcriptomic analyses

Yongping An[1], Qian Wang[2], Yannong Cui[3], Xin Liu[4], Ping Wang[1], Yue Zhou[1], Peng Kang[5], Youjun Chen[1], Zhiwei Wang[2], Qingping Zhou[1] and Pei Wang[1*]

[1] Sichuan Zoige Alpine Wetland Ecosystem National Observation and Research Station, College of Grassland Resources, Institute of Qinghai-Tibetan Plateau, Southwest Minzu University, Chengdu 610225, China
[2] Guizhou Institute of Prataculture, Guizhou Academy of Agricultural Sciences, Guiyang 550006, China
[3] College of Grassland Agriculture, Northwest A&F University, Yangling 712100, China
[4] National Key Laboratory of Crop Genetic Improvement, Ministry of Agriculture Key Laboratory of Crop Ecophysiology and Farming System in the Middle Reaches of the Yangtze River, College of Plant Science and Technology, Huazhong Agricultural University, Wuhan, China
[5] College of Biological Science and Engineering, North Minzu University, Yinchuan 750021, China
* Correspondence: wangpei@swun.edu.cn

ABSTRACT

Siberian wildrye (*Elymus sibiricus*) is a xero-mesophytic forage grass with high nutritional quality and stress tolerance. Among its numerous germplasm resources, some possess superior drought resistance. In this study, we investigated the physiological differences between drought-tolerant genotype (DT) and drought-sensitive genotype (DS) leaves under drought stress. The results showed that under drought stress, DT maintained a lower leaf water potential for water absorption, sustained higher photosynthetic efficiency, and reduced oxidative damage in leaves by efficiently maintaining the ascorbic acid-glutathione (ASA-GSH) cycle to scavenge reactive oxygen species (ROS) compared to DS. Unigene0047636 (*CER1*) may positively regulates the synthesis of very-long-chain (VLC) alkanes in cuticular wax biosynthesis, influencing plant responses to abiotic stresses. Correspondingly, wax monomers content showed significant induction by osmotic stress in DT but not in DS. It is suggested that limiting stomatal and cuticle transpiration under drought stress to maintain higher photosynthetic efficiency and water use efficiency (WUE) is one of the critical mechanisms that confer stronger drought resistance to DT. This study provides new insights into the molecular mechanisms underlying drought tolerance in *E. sibiricus*. The identified genes may provide a foundation for the selection and breeding of drought-tolerant crops.

Keywords: Siberian wildrye; osmotic resistance; differentially expressed genes (DEGs); stress tolerance; ROS; ABA; cuticular wax

Introduction

Drought is the most common abiotic stress that inhibits plant growth and development and poses a serious threat to crop production sustainability [1,2]. Every year, numerous cases of reduced crop productivity due to droughts result in substantial economic losses, presenting a significant challenge for agricultural production [3,4]. Furthermore, with global climate change and the continued rise in greenhouse gas concentrations, droughts have become more frequent, severe, and prolonged than in recent decades [5-7]. Enhancing plant resilience is imperative for agricultural production and environmental sustainability [8]. Therefore, gaining a comprehensive understanding of the molecular mechanisms governing plant responses and adaptations to drought stress and breeding superior varieties with high drought resistance are promising approaches for ensuring global food security and promoting ecological restoration worldwide [9-11].

In general, virtually every aspect of plant physiology, biochemistry, and cellular metabolism is affected by drought stress [12-16]. Drought results in hyperosmotic stress in plant cells, inhibiting root system water absorption, leading to abnormal growth, an imbalance in water relations, and decreased water-use efficiency (WUE) [4,8,17-19]. In addition, drought disrupts ionic homeostasis, osmotic balance, the cell membrane system, and photosynthesis [13,14,20,21]. Drought also leads to a reduction in stomatal conductance, leaf CO_2 assimilation rate, and enzyme activity [13,15,20]. Moreover, the dry environment induced the production of reactive oxygen species (ROS) in biochemical reactions, including superoxide anion ($O_2^{\cdot-}$), hydrogen peroxide (H_2O_2), hydroxyl radical ($HO^{\cdot}$), and singlet oxygen ($^1O_2$) [13,22]. ROS production and consumption are strictly controlled by the antioxidant systems [15,18,20]. Ascorbate and

glutathione play crucial roles in controlling ROS levels in vivo [13]. Under drought stress, the activities of many oxidative protective enzymes, such as superoxide dismutase (SOD), catalase (CAT), ascorbate peroxidase (APX) and glutathione reductase (GR), are altered [3]. However, as the drought progressively worsens, ROS production overwhelms the scavenging function of the antioxidant system, leading to severe cell damage and death [23].

H_2O_2 has been identified as a key signaling molecule that regulates stomatal closure in plants [24,25]. Stomatal closure is the first defense mechanism by which plants respond to drought by preventing transpiration loss, but at the cost of reducing photosynthetic rates [13]. This reduction in photosynthesis can have significant consequences on plant growth under drought conditions. In addition to the ROS pathway, plants regulate stomatal closure through various pathways, including the abscisic acid (ABA) and Ca^{2+} signaling pathways. ABA-mediated stomatal closure is a crucial drought resistance mechanism in plants [26]. Moreover, the cuticle, which is composed of insoluble cutin and waxes, is another factor that limits transpiration under drought stress and serves as an important barrier for plants against various biotic and abiotic stresses [27,28]. Cutin plays a vital role in the prevention of moisture loss [29]. Leaf epidermal wax increases as soil moisture decreases, and the wax layer reduces stomatal conductance, transpiration, and photosynthesis, thereby facilitating plant adaptation to drought conditions [30]. Nonetheless, a recent study in *Populus* revealed no alteration in the overall amount of leaf waxes, but rather an elevation in their transpiration rate due to modifications in their composition [31].

In addition to ROS scavenging and stomatal closure, plants undergo significant alterations in physiological and biochemical metabolism, and regulate root growth and morphology as adaptive responses to drought environments. These adaptations are intricately regulated by multiple signal networks, including signal perception, signal transduction, transcription, translation, and post-translational modifications [2,32-34]. It has been identified that several key components within these signaling networks play pivotal roles in regulating drought responses in various plant species, such as *Arabidopsis*, rice, and maize [35-37]. These components include receptors, phosphatases, kinases, and a wide array of transcription factors (TFs). These TFs encompass those involved in phytohormone signaling, such as PYR/PYL/RCAR (pyrabactin resistance 1/ PYR1-like/regulatory component of ABA receptors), PP2C (clade A type 2C protein phosphatases), SnRK2s/SAPKs (SNF1/AMPK-related protein kinases), calcium-dependent protein kinases (CDPKs), as well as abscisic acid responsive elements binding factor (ABF), abscisic acid responsive elements (ABRE), myeloblastosis (MYB), WRKY, DREB, NAC, and BHLH TFs [8,33,38-42]. However, our knowledge of the genome-wide molecular mechanisms underlying drought tolerance in plants, especially in gramineous crops and forage grasses, remains limited.

Many native grass species grown in arid and semi-arid areas possess special stress tolerance mechanisms and abundant gene resources. Research on these grasses can potentially significantly contribute to the genetic improvement of crop stress resistance, thereby benefiting agriculture and animal husbandry. Siberian wildrye (*Elymus sibiricus*), a typical perennial meso-xerophytic forage grass widely distributed at high altitudes worldwide, offers good forage quality and environmental adaptability. It is extensively used in natural grasslands, cultivated pastures, and the ecological restoration of degraded grasslands [43-46]. Furthermore, *E. sibiricus* exhibits remarkable resistance to barren conditions, drought, cold, salinity, and diseases [45,47]. However, despite its impressive resilience, the mechanisms underlying its drought tolerance remain poorly understood.

In our previous study, we screened drought-tolerant (DT, I-1-1-46) and drought-sensitive (DS, I-1-1-2) genotypes of *E. sibiricus*, and revealed that the Casparian strip and suberin lamellae in the root endodermis played a pivotal role in the difference in drought resistance between the DT and DS genotypes [48]. Here, we performed a comparative analysis of the physiological, biochemical and transcriptomic changes in the leaves of DT and DS genotypes in response to drought stress to clarify two major issues: (1) What are the differences in the physiological responses to drought stress in the leaves of different genotypes? (2) What is the molecular basis underlying the distinct drought tolerances of the two genotypes? The results of this study are expected to shed new light on the understanding of plant drought resistance, offering potential pathways for the development of more drought-tolerant forage grass and crop cultivars through molecular breeding methods.

Results

Effects of drought on leaf water status in DT and DS

Under the control condition (75% field water content [FWC]), there was no significant differences in leaf water potential (Ψ_w), osmotic potential (Ψ_s) and turgor pressure (Ψ_t) between DT and DS (Table 1). As drought intensity increased, Ψ_w and Ψ_s decreased significantly in both DT and DS leaves. However, they were remarkably lower in DT than in DS under moderate (45% FWC) and severe (30% FWC) drought stress (Table 1). Under mild drought stress (60% FWC), although there was no significant difference in Ψ_w between the two genotypes, Ψ_s of DT was significantly lower than that of DS (Table 1). With the exacerbation of drought stress, Ψ_t in both genotypes initially increased and then decreased, and it was significantly lower in DT than in DS under severe drought stress (Table 1). These results indicate that *E. sibiricus* can absorb water from drought soils by reducing the osmotic potential and, consequently, water potential, with DT exhibiting a more advantageous capacity in this regard.

Table 1. Effects of drought on leaf water status of two *E. sibiricus* genotypes.

Genotype	Moisture gradient Field water content (FWC) %	Water potential Ψ_w (Mpa)	Osmotic potential Ψ_s (Mpa)	Turgor pressure Ψ_t (Mpa)
DT	75	-0.82±0.04 f	-1.29±0.01 f	0.46±0.03 d
	60	-1.19±0.04 e	-1.99±0.02 d	0.80±0.03 b
	45	-2.06±0.04 c	-2.98±0.01 b	0.91±0.03 a
	30	-2.83±0.06 a	-3.18±0.06 a	0.35±0.13 e
DS	75	-0.82±0.04 f	-1.27±0.01 f	0.45±0.03 d
	60	-1.19±0.04 e	-1.85±0.02 e	0.66±0.06 c
	45	-1.98±0.02 d	-2.89±0.03 c	0.92±0.04 a
	30	-2.53±0.08 b	-2.99±0.03 b	0.46±0.05 d

Note: Values are presented as the means ± standard deviation (SD) (n=6) and bars indicate SD; columns with different letters indicate significant differences at $P < 0.05$ (Duncan's test). DT, drought-tolerant genotype; DS, drought-sensitive genotype; FWC: field water content.

Effects of drought stress on photosynthesis of two E. sibiricus genotypes

Under the control conditions, there were no significant differences in net photosynthetic rate (Pn), stomatal conductance (Gs), and water use efficiency (WUE) between DT and DS, whereas the transpiration rate (Tr), intercellular carbon dioxide concentration (Ci), and limiting value of stomata (Ls) in DT were significantly higher than those in DS (Figure 1). As soil water content decreased, Ci increased dramatically, whereas the other five photosynthetic indices decreased markedly in both genotypes (Figure 1). Overall, under drought stress, DT consistently exhibited higher values for all six photosynthetic indices compared to DS. The most pronounced differences were observed under severe drought stress, where DT had a 46, 30, 17, 19, and 13% higher Pn, Gs, WUE, Ls, and Ci than DS. Notably, at this point, the Tr of the DT leaves was was not significantly higher than that of the DS leaves (Figure 1).

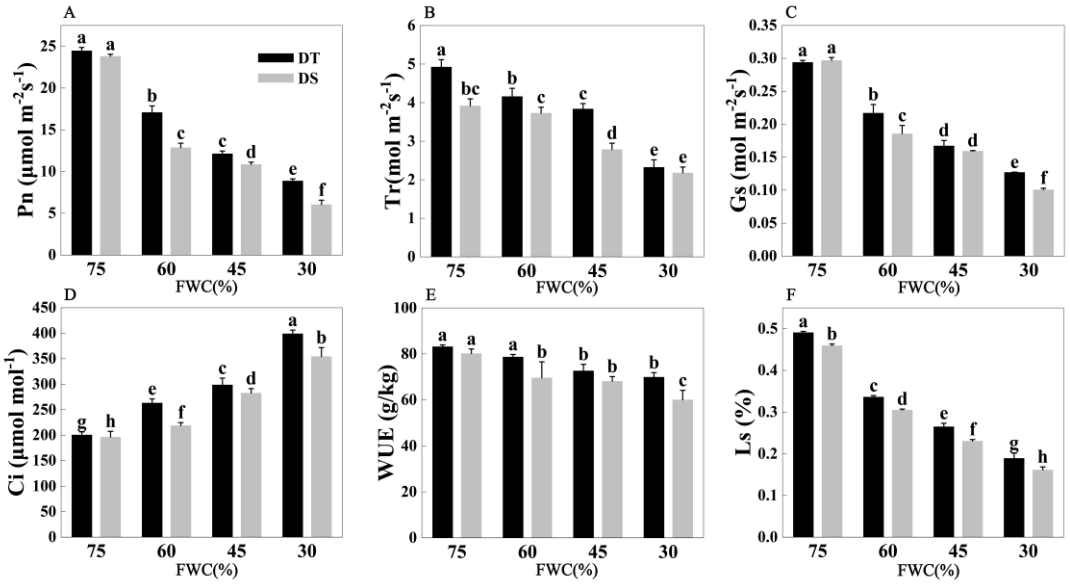

Figure 1. Responses of leaf photosynthetic characteristics in two *E. sibiricus* genotypes to drought stress. (**A**) Net photosynthetic rate (Pn); (**B**) transpiration rate (Tr); (**C**) stomatal conductance (Gs); (**D**) intercellular carbon dioxide concentration (Ci); (**E**) water use efficiency (WUE); (**F**) limiting value of stomata (Ls). The data are presented as the means of three replicates (± SD) based on Duncan's multiple range test. Means denoted with the same letter indicates no significance ($P > 0.05$). DT, drought-tolerant genotype; DS, drought-sensitive genotype.

Differences in leaf ROS accumulation and ascorbate-glutathione cycling in drought responses

The superoxide anion radical ($O_2^{\cdot-}$) content did not significantly differ between DT and DS in either the control or mild to moderate drought stress (≥ 45% FWC). However, under severe drought stress, the $O_2^{\cdot-}$ content in DS was notably higher (38%) than that in DT (Figure 2A). Hydrogen peroxide (H_2O_2) levels in both DT and DS leaves increased with decreasing soil water content. DT had significantly lower levels of H_2O_2 than DS under moderate to severe drought (≤ 45% FWC) (Figure 2B). Glutathione (GSH) and ascorbic acid (ASA) are important antioxidants involved in ROS scavenging. There was little difference in GSH content between DT and DS across the 30–75% drought gradient (Figure 2C). However, ASA content increased with increasing drought intensity and was significantly higher in DT than in DS under mild to severe drought stress (Figure 2D).

Therefore, we analyzed ASA-related indices, including mono-dehydroascorbic acid reductase (MDHAR), dehydroascorbate reductase (DHAR), ascorbate peroxidase (APX), and the ratio of ascorbic acid to dehydroascorbic acid (ASA/DHA). The results showed that the MDHAR, DHAR, and ASA/DHA contents continuously increased with increasing drought intensity (Figure 2E, F, H), whereas the APX content initially decreased drastically and then slightly increased (Figure 2G). In the control treatment (75% FWC), the contents of MDHAR, DHAR, and ASA/DHA were not significantly different between DT and DS, whereas the APX content was significantly higher in DT than in DS (Figure 2 E-H). The MDHAR content was significantly higher in DT than in DS under severe drought stress, but there was no significant difference between them in the remaining treatments (Figure 2E). The DHAR, APX contents and ASA/DHA of DT were significantly higher than those of DS under all drought treatments (Figure 2F-H). These findings highlight the importance of ASA in the response of DT to drought stress.

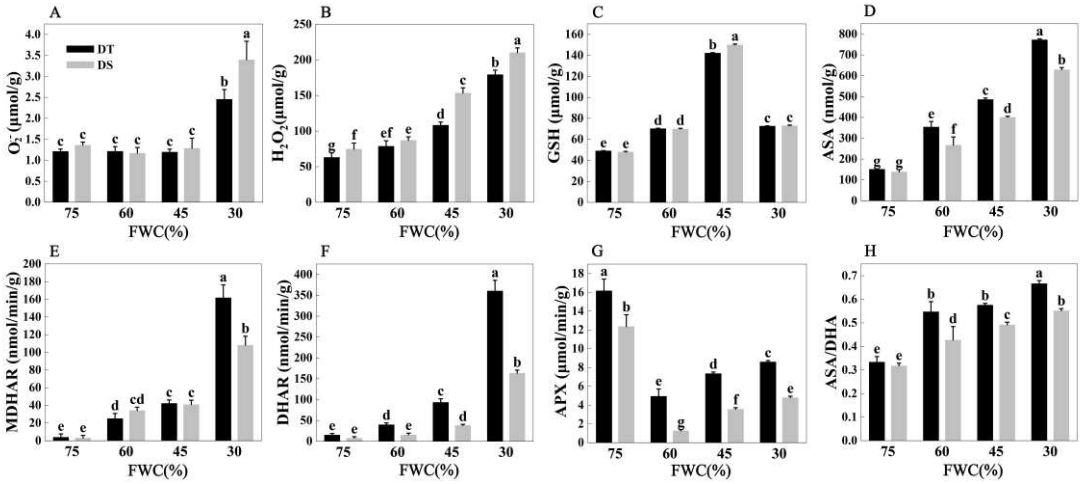

Figure 2. Responses of leaf ascorbic acid-glutathione cycle in two *E. sibiricus* genotypes to drought stress. (**A**) Superoxide anion radical ($O_2^{\cdot-}$); (**B**) hydrogen peroxide (H_2O_2); (**C**) glutathione (GSH); (**D**) ascorbic acid (ASA); (**E**) mono-dehydroascorbic acid reductase (MDHAR); (**F**) dehydroascorbate reductase (DHAR); (**G**) ascorbate peroxidase (APX); (**H**) ascorbic acid/dehydroascorbic acid (ASA/DHA). The data are presented as the means of three replicates (± SD) based on Duncan's multiple range test. Means denoted with the same letter indicate no significance $P > 0.05$. DT, drought-tolerant genotype; DS, drought-sensitive genotype.

Transcriptome analysis of DT and DS in response to osmotic stress

Libraries were constructed and sequenced on an Illumina HiSeq™ 4000 deep sequencing platform, and detailed RNA sequencing results are shown in Supplementary Table S1. Clean reads were assembled to obtain 136,699 unigenes; detailed information on the evaluation indicators can be found in Table S2. These unigenes were annotated in four protein databases: 80,610 in Nr, 67,301 in KEGG, 31,763 in COG, and 39,932 in SwissProt (Table S3 and Figure S1). The RNA-seq data were credible and reproducible using PCA and Pearson's correlation coefficient analyses (Figures S2, and S3).

Volcano plots identified significantly upregulated or downregulated genes during osmotic stress at each time point (Figure 3A-D). In DT, there were 3,002 DEGs (1,664 upregulated and 1,338 downregulated) and 2,464 DEGs (986 upregulated and 1,478 downregulated) were observed at 3 and 24 h, respectively, compared with the control (Figure 3E). In DS, there were 1,555 DEGs (481 upregulated and 1,074 down-regulated) at 3 h and 1,691 DEGs (873 upregulated and 818 down-regulated) at 24 h compared with the control (Figure 3E). Venn diagrams displayed the number of common and uniquely expressed unigenes at both time points (Figure 3F-H), 2,234 and 1,696 DEGs were unique in DT at 3 and 24 h, respectively, compared to the control (Figure 3F), whereas 900 and 1,036 DEGs were uniquely expressed in DS at 3 and 24 h, respectively, compared with the control (Figure 3G). In addition, 768 and 655 DEGs were common at both time points for both DT and DS, respectively (Figure 3F, G), indicating that a higher number of unigenes were regulated in DT than in DS. Further analysis revealed 197 DEGs were co-expressed in DS and DT (Figure 3H).

GO enrichment analysis of the upregulated and downregulated genes revealed key GO term associated with osmotic stress. GO enrichment for DEGs was higher in DS than in DT, the number of genes annotated to GO was higher in DS (fg_num=1380) than in DT (fg_num=978) (Figure S4 and Table S4). DS and DT are mainly enriched in the two GO terms associated with hydrolase activity in molecular function, hydrolase activity, acting on glycosyl bonds (GO:0016798) and hydrolase activity, hydrolyzing O-glycosyl compounds (GO:0004553), respectively (Figure S4 and Table S4). Using the KEGG database to investigate the key genes involved in the KEGG pathways, these DEGs were found to be significantly enriched in plant hormone signal transduction (ko04075), biosynthesis of secondary metabolites (ko01110), and the MAPK signaling pathway (ko04016) (Figure S5 and Table S5).

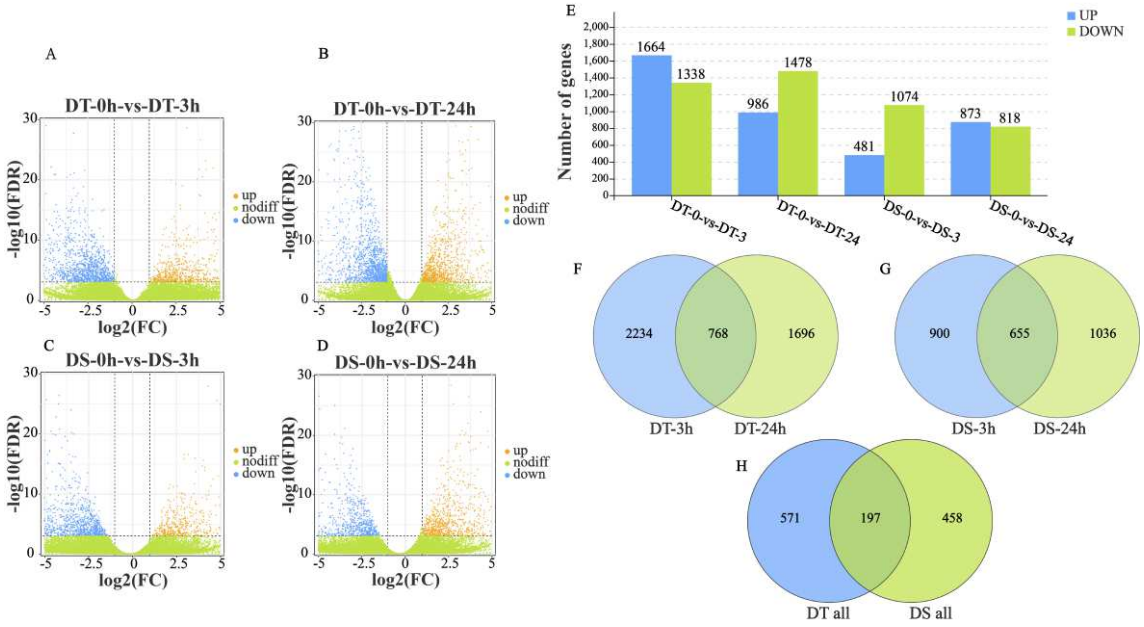

Figure 3. Analysis of differentially expressed genes in *E. sibiricus* genotypes in response to osmotic stress. (**A-D**) Volcano plots of all expressed genes in drought-tolerant (DT) and drought-sensitive (DS) genotypes at different time points compared to the control (CK), with $\log_2$FC values drawn against $-\log_{10}$ (FDR) adjusted *P*-values. Orange and blue dots represent upregulated and downregulated DEGs based on $|\log_2(\text{foldchange})| \geq 2$ and FDR ≤ 0.001; green dots represent non-significant DEGs; (**E**) number of upregulated and downregulated DEGs identified under different osmotic-stress treatments compared to the control DT and DS; (**F**) common and unique DEGs under 3 and 24 h osmotic-stress treatments in DT; (**G**) common and unique DEGs under 3 and 24 h osmotic-stress treatments in DS; (**H**) common and unique DEGs under both 3 and 24 h osmotic-stress treatments in DT and DS.

Screening of differential candidate genes in DT and DS under osmotic stress

We performed hierarchical clustering for 1,226 DEGs ($\log_2$FC value) in response to osmotic stress in the two *E. sibiricus* genotypes (Figure 3H). The heat map identified two clustering modules for the DEGs. Cluster1 consists of 833 DEGs that exhibited high expression levels in DT and DS under normal conditions, but low expression levels under osmotic stress. In contrast, cluster2 includes 393 DEGs that showed the opposite expression trend compared to cluster1 (Figure 4A). Further analysis of cluster1 identified five notable trend blocks linked to profiles 3, 10, 2, 6, and 0, with 212, 167, 153, 134, and 95 unigenes, respectively. Additionally, cluster2 exhibited four significant trend blocks attributed to profiles 9, 16, 17, and 13, comprising 118, 115, 55, and 54 unigenes, respectively (Figure 4B, C).

To efficiently screen the candidate genes for DT osmotic tolerance, we focused on profile 16 of cluster2. A total of 115 DEGs in the DT and DS genotypes exhibited low expression levels without stress treatment. However, DT was highly induced compared to DS in the early stages of the 3-h osmotic stress treatment, and both were highly expressed in the 24-h stress treatment (Figures 4C and 5A). Heatmap analysis showed that the expression of 115 DEGs in profile 16 was higher in the DT genotype DT than in the DS genotype under osmotic stress (Figure 5B). Eight candidate unigenes that were highly expressed specifically in DT under osmotic stress were screened from 115 DEGs: Unigene0005863 (*EsSnRK2*), Unigene0047636 (*EsCER1*), Unigene0005889 (*EsGOLS1*), Unigene0066379 (*EsCAD8D*), Unigene0005868 (*EsSAHH*), Unigene0031985 (*EsCIPK5*), Unigene0041137 (*EsAZF2*), and Unigene0053902 (*EsLRK10*) (Figure 5C). The expression of these eight candidate genes in DT was significantly upregulated under osmotic stress, whereas they remained unchanged in DS in response to osmotic stress. These candidate unigenes were enriched in cutin, suberin, and wax biosynthesis, galactose metabolism, cysteine and methionine metabolism, MAPK signaling pathway, plant hormone signal transduction, phenylpropanoid biosynthesis, biosynthesis of secondary metabolites and metabolic pathways (Figure 5D). Among these, Unigene0005863 (*EsSnRK2*) encodes a key protein kinase in the MAPK and plant hormone (ABA)

signal transduction pathways (Figures S7, and S8). In addition, our study found that unigenes associated with ROS scavenging in the ASA-GSH system were differentially expressed in DT and DS (Figure S9).

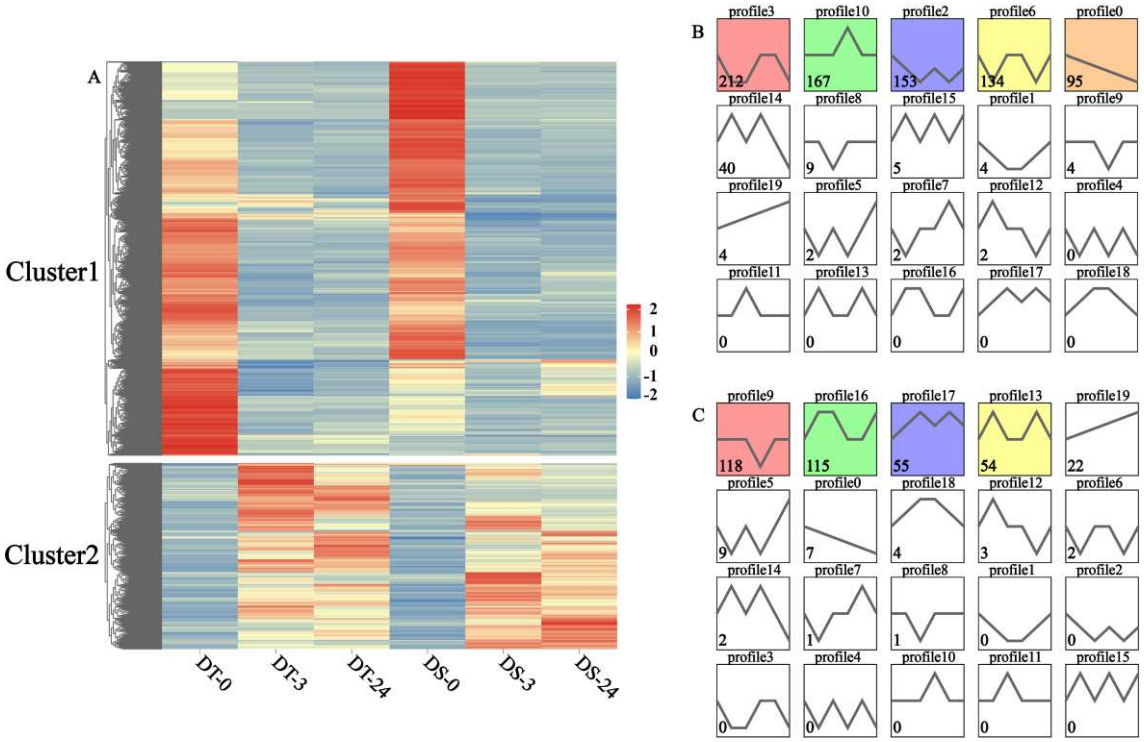

Figure 4. Clustering and trend analysis of differentially expressed genes (DEGs) in DT and DS genotypes under osmotic stress. (**A**) Hierarchical clustering analysis indicates DEG expression patterns in DT and DS after 0, 3, and 24 h of osmotic stress treatment; (**B-C**) trend analysis shows that the lines reflect expression patterns for each DEG at osmotic stress time points. Black lines in each trend blocks indicate mean changes in DEG expression. The different profiles represent the numbers of the different trend blocks, and the numbers within the trend blocks indicate the number of enriched genes. Trend blocks with color are significantly enriched (p<0.05), while trend blocks without color are not significantly enriched. Each inflection point represents a set of sample data.

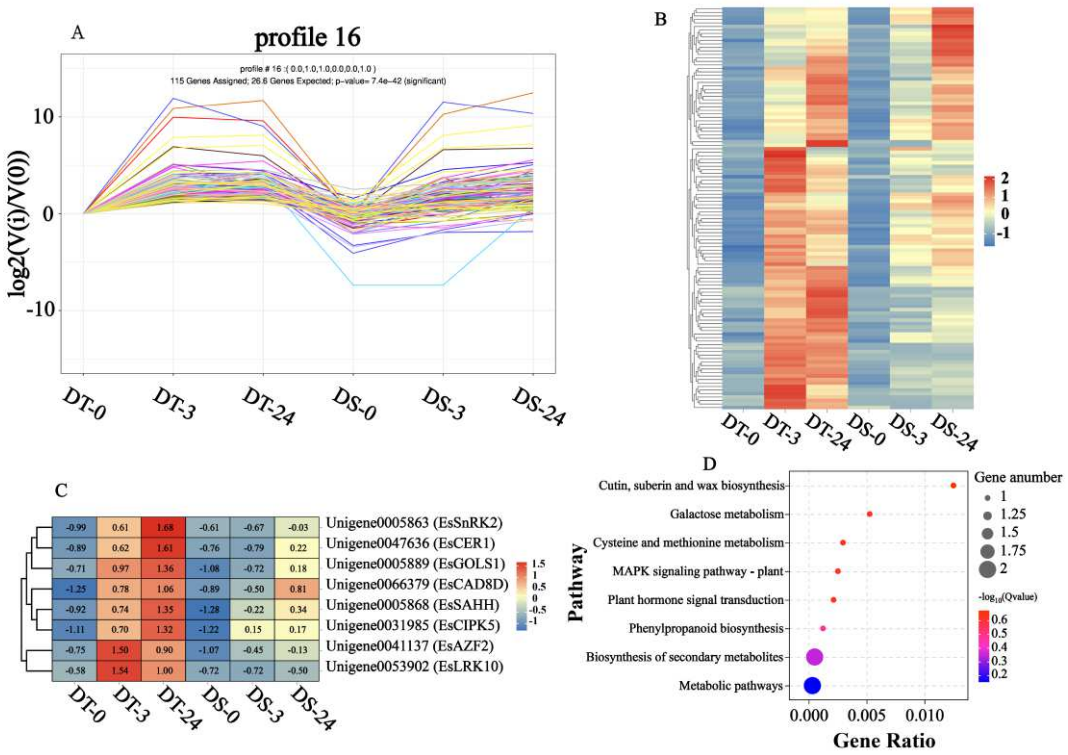

Figure 5. The trend analysis plots, expression heatmap, and enrichment bubble plots of DEGs in DT and DS genotypes at different time points. (**A**) Trend analysis graph for DT and DS in profile 16 trend block; (**B**) heatmap of DT and DS expression in the profile 16 trend block; (**C**) heatmap expression of candidate genes; (**D**) enrichment bubble map of candidate genes.

Effects of osmotic stress on leaf cuticular wax and cutin monomer contents

Among the DEGs presented in Figure 5C, we noted that Unigene0047636, a homologous gene of CER1 in *Arabidopsis* through sequence alignment which may encode an enzyme involved in forming alkane monomers during wax biosynthesis, was significantly induced by osmotic stress in DT, but not in DS (Figure S6). Therefore, we analyzed the cuticular wax and cutin monomer contents. Results showed that there was little difference in the wax and cutin monomer contents between the two genotypes without osmotic stress (Figure 6A, B). However, osmotic stress (20% PEG-6000) significantly increased the content of alkanes, alcohols, and aldehydes in the wax monomers of DT, without increasing any monomers in DS, resulting in the three major wax monomers being higher in DT than in DS under osmotic stress (Figure 6A). However, only one DEG, Unigene0047636 (*CER1*), was detected in the wax biosynthesis pathway (Figure 6C), suggesting that *CER1* may be a key factor in wax biosynthesis in the DT response to osmotic stress. In addition, although osmotic stress slightly increased the contents of some cutin monomers in DT, such as alcohols, ω-OH fatty acids, and polyhydroxy fatty acids (PFAs), which were not induced by osmotic stress in DS, transcriptome sequencing did not detect any DEGs between the two genotypes in the cutin biosynthesis pathway (Figure 6B, D).

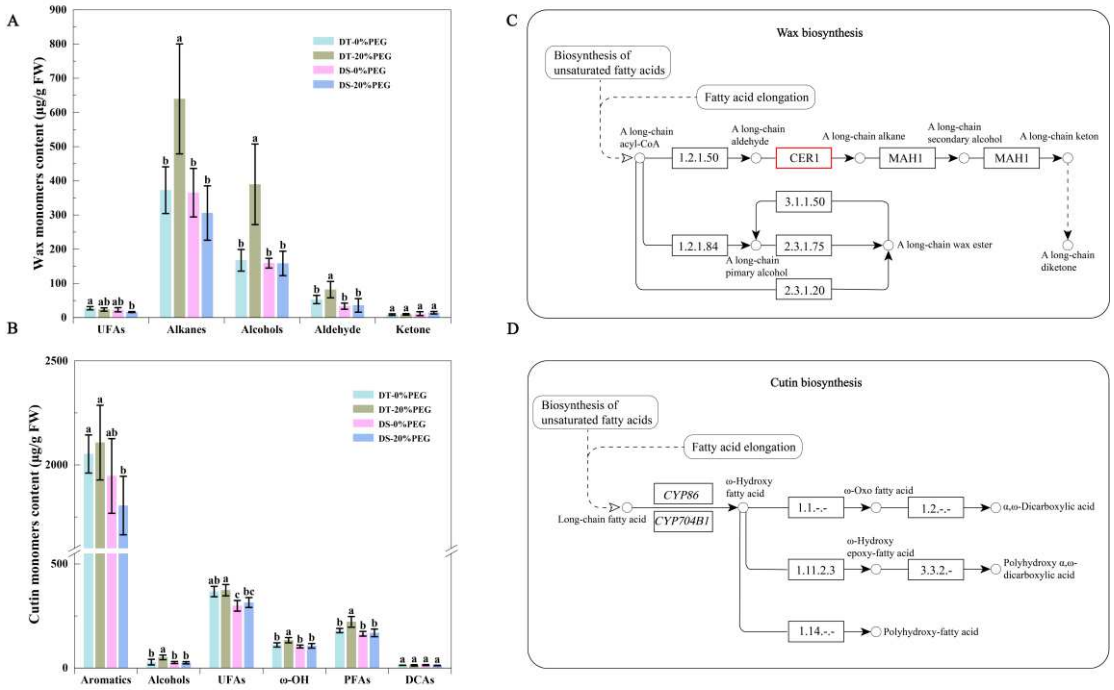

Figure 6. Difference in leaf cuticle between DT and DS genotypes under osmotic stress. (**A**) Wax monomers content; (**B**) Cutin monomers content; (**C**) Wax biosynthesis pathway; (**D**) Cutin cutin biosynthesis pathway. Wax and cutin data are presented as the means ± SD based on Duncan's multiple range test. Means denoted with the same letter indicate nonsignificance ($P > 0.05$). DT, drought-tolerant genotype; DS, drought-sensitive genotype. The genes with red borders are up-regulated genes in the KEGG pathway.

Discussion

The drought tolerance of plants is strongly related to their ability to use' water [17]. The difference in the water potential gradient between the inside and outside of plant cells is the key to water transport across the membrane [49]. Under drought stress, plants can reduce cellular water potential through osmoregulation to maintain the water potential difference between the root system and the soil environment, and to absorb water from dry soils with low water potential [50]. Under drought stress, DT had a lower leaf Ψ_w and Ψ_s than DS (Table 1), which indicated the higher drought resistance of DT. Furthermore, our results showed that the Ψ_t of DT was significantly lower than that of DS under severe drought stress (Table 1). Cell turgor pressure plays a pivotal role in governing the stomatal aperture, with reduced turgor pressure predominantly leading to stomatal closure [51]. However, the Gs of DT was significantly higher than that of DS, corresponding to a higher Pn of DT than that of DS (Figure 1A, C), indicating a higher photosynthetic capacity of DT. In addition, Ci and WUE of DT were higher than those of DS under different drought stress treatments (Figure 1D, E). The factors causing reduced photosynthesis under drought stress can be divided into two categories: stomatal limitation and non-stomatal limitation; the former is due to a limitation of Gs, causing Ci to fail to meet photosynthetic demand, and the latter is due to reduced chloroplast and photosynthetic enzyme activities [52,53]. In the present study, the Gs of both genotypes gradually decreased with increasing drought intensity, whereas the Ci gradually increased and Ls decreased (Figure 1C, D). This result indicated that the stomatal limitation of *E. sibiricus* gradually decreased with increasing drought intensity, and the factors leading to the inhibition of photosynthesis gradually changed to non-stomatal limitation.

In response to osmotic stress, plants control water balance through stomatal movement [54]. Plants employ multiple pathways to close stomata under drought stress, with the ABA signaling pathway being one of the most crucial mechanisms [26]. In addition to the ABA signaling pathway, other signaling pathways, such as ROS, can also regulate stomatal opening and closure during drought stress [55]. These mechanisms work synergistically to reduce water transpiration and enhance drought tolerance [56]. Our transcriptome study screened eight DEGs involved in the response of *E. sibiricus* to osmotic stress, which were significantly upregulated in DT,

but not in DS, under osmotic stress (Figure 5C). Among these eight genes, Unigene0005863 (*EsSnRK2*), Unigene0053902 (*EsLRK10*) and Unigene0031985 (*EsCIPK5*) may be involved in stomatal closure induced by the ABA signaling pathway. *SnRK2* is a key protein kinase involved in the ABA signal transduction pathway, which regulates stomatal closure to prevent leaf water loss in *Arabidopsis* [57]. The wheat *SnRK2s* family member *TaSnRK2.1* is Involved in stomatal closure, osmotic regulator biosynthesis, cellular ROS scavenging, homeostasis, and other stress-related biological processes during drought stress and ABA induction [58]. Unigene0053902 (*EsLRK10*) is homologous to *LPK10L1.2* in *Arabidopsis*. *Arabidopsis* mutants lacking *LPK10L1.2* exhibit ABA-insensitive and drought-sensitive phenotypes [59]. *CdtCIPK5* from *Cynodon dactylon* (L.), the homologous gene of Unigene0031985 (*EsCIPK5*), is induced by multiple abiotic stresses such as ABA, dehydration, low temperature, and salt stress [60]. The high expression of these eight candidate genes in DT under osmotic stress may be the key to its drought resistance, but how they regulate drought resistance at the molecular level in *E. sibiricus* DT genotypes requires further study.

Plant cuticular waxes, primarily composed of very-long-chain (VLC) aliphatic lipids, such as alkanes, aldehydes, primary and secondary alcohols, ketones, and esters, serves as a crucial barrier for plants against environmental stresses [27,61]. These waxes, located in the leaf epidermis, are believed to mitigate water loss during drought stressand contribute to the reduction of stomatal conductance, transpiration rates, and photosynthesis, thereby enhancing drought resistance of plants [29,30]. This protective function is particularly important in xerophytes. Our results indicated a notable increase in wax content under osmotic stress in DT, as opposed to DS. However, Shellakkutti et al.[62] discovered that osmotic stress in both cultivated and wild barley led to an increase in wax crystals accumulation, total wax amounts, and wax gene expression, while cuticular conductance remained unaffected. Similarly, a recent study in *Populus* revealed that alterations in the compositions of wax, despite without altering the total amounts, led to elevated transpiration rates[31]. Alkanes, the predominant constituents of plant cuticle waxes [63], are thought to play a crucial role in conferring drought tolerance [64]. Grünhofer et al.[31] pinpointed a rise in the relative proportion of esters in the *Populus* × *canescens cer6_1,2* mutant as the primary factor to the heightened transpiration rate, in fact, alkanes in the mutant decreased significantly. Notably, our results showed that the content of alkane, alcohol, and aldehyde monomer in DT was significantly higher than that in DS (Figure 6A), suggesting that DT may enhance drought tolerance by accumulating more wax alkanes.

Wax biosynthesis is regulated by multiple genes encoding enzymes and transporters necessary for the deposition of cuticle constituents [65]. Among these genes, *CER1* plays a pivotal role in the drought stress-induced biosynthesis of cuticular wax [66,67]. In a study on alkane synthesis in wheat epidermal waxes, researchers found that *TaCER1-1A*, a *TaCER1* homolog, increased the alkane contents in both transgenic rice and *Arabidopsis,* leading to an improved epidermal barrier and enhanced drought tolerance in the leaf epidermis of transgenic lines [68]. Additionally, *TaCER1-6A* is a crucial gene in wheat, significantly involed in alkane biosynthesis. Knockout mutants of *TaCER1-6A* exhibited reduced alkane contents in their leaves, whereas overexpression of *TaCER1-6A* increased alkane contents, thereby improving drought tolerance in wheat [64]. Furthermore, in tomato and *Poa pratensis*, the *SlCER1-1* and *PpCER1-2*, respectively, positively regulate the synthesis of wax alkanes, reducing cuticle permeability and enhancing drought tolerance[69,70]. Wen et al.[71] found that the downregulation of two *TaCER1* genes led to decreased long-chain alkanes synthesis in low-wax wheat mutants. Our results showed that the expression of Unigene0047636, homologous to *CER1*, was upregulated in DT but remained unchanged in DS under drought stress (Figure 5C). Harb et al.[72] found that in barley, *HvCER1* was specifically induced under drought stress in the drought-tolerant genotype, but not in the drought-sensitive genotype, which is consistent with our results. Drought stress caused a significant increase in very-long-chain alkanes in the wax components of *Brachypodium distachyon*. *BdCER1-8*, homologous gene of *CER1*, is highly expressed in leaves [73]. In *Arabidopsis*, *CER1* encodes an alkane-forming enzyme that catalyses the decarbonylation of aliphatic aldehydes to alkanes [74]. Therefore, we hypothesized that *EsCER1* positively regulates the conversion of long-chain aldehyde monomers to long-chain alkane monomers during wax biosynthesis, which may be an important reason for the difference in drought resistance among the different genotypes of *E. sibiricus*.

The reactive oxide species (ROS) are essential signaling molecules in various physiological processes, playing a crucial role in regulating plant growth and development [75]. However, excessive ROS accumulation can be toxic to plants and can lead to oxidative damage [76,77]. To counteract ROS toxicity, plants possess a complex detoxification system, that includes a non-enzymatic

ASA-GSH pathway [78]. The ASA-GSH pathway serves as a vital component in reducing oxidative damage by scavenging ROS through the detoxification mechanisms of ASA, GSH, and their associated enzymes [79,80]. The ASA-GSH cycle is comprised of four key enzymes: ascorbate peroxidase (APX), mono-dehydroascorbate reductase (MDHAR), dehydroascorbate reductase (DHAR), and glutathione reductase (GR) [80]. In the present study, we observed a lower overall level of ROS ($O_2^{\cdot-}$ and H_2O_2) accumulation in DT compared to DS during drought stresses (Figure 2A-B). Further studies revealed that the ASA, DHAR, and APX content in the DT was higher than that in the DS (Figure 2D, F, G). The above studies suggest that the greater drought tolerance of DT compared to DS may be due to its ability to maintain lower ROS levels through higher ASA, DHAR, and APX concentrations in the ASA-GSH cycle.

APX1 and APX2 are cytoplasmic enzymes that play crucial roles in ROS scavenging [81,82]. Previous studies have demonstrated their significance in mitigating the ROS levels in plants. For instance, in a study on ROS accumulation in *Arabidopsis*, it was found that the overexpression of *APX1* and *APX2* resulted in a significant decrease in ROS levels [83]. Research on *Stevia rebaudiana* has demonstrated that the plant's response to abiotic stress involves the upregulation of key genes encoding ROS-scavenging enzymes such as glutathione S-transferase (GST) and APX, contributing to the modulation of its stress response[84]. Under osmotic stress, RNA-seq results revealed that genes relevant to the ASA-GSH cycle (APX, GR, DHAR, and GST) were differentially expressed in DT and DS (Figure S9). In addition, the overall expression of Unigene0106502 (*EsAPX1*), Unigene0005132 (*EsAPX2*), Unigene0013814 (EsGR1) and Unigene0023285 (EsGST4) were higher in DT than in DS (Figure S9). These findings may suggest a potential role for these unigenes in the regulation of ROS accumulation in DT and DS.

Materials and Methods

Plant Materials and Treatments

Two genotypes (DT and DS) of *E. sibiricus* were used in this study [48]. Plant materials used to determine physiological phenotypes were grown in soil, materials for cutin, wax and transcriptome sequencing were cultured by hydroponics.

For soil culture: Seeds were vernalized for 3 d in the dark at 4 ℃, then germinated on wet filter paper. After 2 d, the seedlings were transferred to pots (diameter, 10 cm; depth, 8.5 cm; 9 seedlings/pot) containing peat soil, and incubated at 23 and 19 ℃ during the day and night, respectively, with 16 h of light, and 40–60% relative humidity. A compound fertilizer with a 1:1:1 N:P:K ratio was applied every 2 d. After 10 d, when the plants reached the third-leaf stage, they were divided into four experimental groups: (1) control: watered with distilled water until water content was maintained at 75% of the field water content (FWC) by weight; (2) mild drought treatment: stopped watering until water content of the medium decreased to 60% FWC, and distilled water was used to maintain this content; (3) moderate drought treatment: maintained at 45% FWC; (4) severe drought treatment: maintained at 30% FWC. The FWC was calculated by assessing the moisture level of the peat soil using a cutting ring technique. Correlation indices were measured after 12 d of treatment, and six biological replicates were used for each treatment (three plants/replicate).

In hydroponics, seed germination was the same as that observed in the soil culture experiment. Two days after germination, the seedlings were transferred to hydroponic boxes filled with half-strength Hoagland solution (H353, Phyto TechLabs, Lenexa, KS, USA), which was aerated using an air pump. The environmental conditions in the climatic chamber were consistent with those of the soil culture. Subsequently, 28-day-old seedlings were treated as follows: (1) Seedlings were transferred to half-strength Hoagland solution containing 0 (control) or 20% PEG-6000 (BioFroxx, Einhausen, Germany) for 3 d. Cutin and wax of the leaf tissue were then measured after harvest. Each treatment consisted of six biological replicates. (2) seedlings were transferred to half-strength Hoagland solution containing 20% PEG-6000 and treated for 0, 3, and 24 h. Fresh leaves were then collected, immediately frozen in liquid nitrogen and stored at –80℃ for transcriptome sequencing. Each treatment had three biological replicates.

Measurement of leaf water potential, osmotic potential and turgor pressure

The leaf water potential (Ψ_w) was measured using a water potential meter (PSYPRO; DIANJIANG TECH, USA). For the osmotic potential (Ψ_s), leaf samples (0.5 g) were washed with deionized water, dried with filter paper, and immediately frozen in liquid nitrogen. Subsequently, the samples were placed in a syringe the sap was squeezed out. The sap was then centrifuged, and 50

μL of the supernatant was used to measure the ic value with a freezing point osmometer (OSMOMAT 3000, Gonotec GmbH, Germany). Ψ_s was calculated according to the formula:

Ψ_s= -icRT.

where R is the gas constant 0.008314 and T is the measured thermodynamic temperature (298.8 K). The turgor pressure (Ψ_t) is calculated according to the formula:

$\Psi_t = \Psi_w - \Psi_s$.

Measurement of photosynthetic parameters

Photosynthetic parameters were measured using a portable photosynthesis system instrument (LI-6800, LI-COR Biosciences, USA). To ensure that the plants received sufficient light before measurement. The measurements were conducted between 8:00–11:30 am. The photosynthetic system parameters were set as described below: leaf chamber area of 2 cm^2, photosynthetic effective radiation of 1000 lx, and temperature of 25 ℃. The following photosynthetic indicators were measured: the net photosynthetic rate (Pn), stomatal conductance (Gs), transpiration rate (Tr), and intercellular carbon dioxide concentration (Ci). Based on the above measured indices, the water use efficiency was calculated according to the formula: WUE = Pn/Gs [85] and the limiting value of stomata (Ls) was calculated using the formula: Ls = (Ca-Ci)/Ca [86], where Ca is the atmospheric carbon dioxide concentration.

Determination of ROS and antioxidant contents

Plant leaves (0.1 g) were used to measure the content of ROS ($O_2^{\cdot-}$ and H_2O_2) in the control and drought treatment groups using $O_2^{\cdot-}$ and H_2O_2 kits, respectively. Ascorbic acid (ASA), glutathione (GSH) and dehydroascorbic acid (DHA) levels were determined using ASA, GSH and DHA kits, respectively. The activity levels of circulatory metabolism-related enzymes, including dehydroascorbate reductase (DHAR), monodehydroascorbic acid reductase (MDHAR) and ascorbate peroxidase (APX), were measured using DHAR, MDHAR and APX kits, respectively. All the kits were obtained from Suzhou Comin Biotechnology Co., Ltd. (Suzhou, China). The measurement of these indices were performed according to the manufacturer's instructions.

Determination of cutin and wax contents

Leaves were used to determine the cutin and wax content. Cutin monomers were extracted via tissue delipidation, ester depolymerization, and silylation, as described by Jenkin and Molina [87]. Waxes were determined as follows: leaf tissues were extracted by placing leaves in 10 mL of chromatographically pure chloroform for 30 s; 25 μL C24 alkane (1 μg/μL) was added as an internal standard, then the solutions were blow-dried with nitrogen, silylated with 100 μL of N, O Bis-trimethylsilyl-trifluoroacetamid (BSTFA) and 100 μL of pyridine for 30 min at 100 ℃, and blow-dried with nitrogen again, and finally dissolved in 100 μL of hexane.

The cutin and wax monomer contents were determined using a gas chromatograph-mass spectrometer (GC-MS; 8890-7000D, Agilent Technologies, USA) fitted with an HP-5MS capillary column (length, 30 m; i.d., 0.25 mm; film thickness, 0.25 mm). For cutin, the injector was set at 250 ℃, and the injected split ratio was 1:10 and helium was the carrier gas at a constant flow rate of 1.5 mL min^{-1}. The oven was initially set at 50 ℃ for 2 min, increased by 40 ℃ min^{-1} increments to 200℃, maintained for 5 min, then increased by 5 ℃ min^{-1} increments to 310 ℃, and maintained for 20 min. The temperature of the MS detector was 325 ℃, and the MS was set to scan mode > 40–600 amu (electron impact ionization). For wax, the injector was set at 250 ℃, the oven was initially set at 80 ℃ for 1 min, increased by 15 ℃ min^{-1} increments to 260 ℃, maintained for 10 min, then increased by 5 ℃ min^{-1} increments to 320 ℃, and maintained for 24 min. The temperature of the MS detector was 320 ℃, and the MS was set to scan mode > 40–600 amu. Six biological replicates were assessed in each experiment.

RNA extraction, library construction and sequencing

Total RNA was extracted using a TRIzol reagent kit (Invitrogen, Carlsbad, CA, USA) according to the manufacturer's instructions. The RNA quality was assessed using an Agilent 2100 Bioanalyzer (Agilent Technologies, Palo Alto, CA, USA) and verified using RNase-free agarose gel electrophoresis. Conventional kits were used to remove rRNA and enrich mRNA. The

enriched mRNA was then cut into short fragments using a fragmentation buffer and reverse transcribed into cDNA using random primers. The cDNA fragments were purified using the QiaQuick PCR extraction kit (Qiagen, Venlo, Netherlands), end-repaired, poly(A) added, and ligated to Illumina sequencing adapters. The ligation products were size-selected by agarose gel electrophoresis, PCR-amplified, and sequenced using an Illumina HiSeqTM 4000 by Gene Denovo Biotechnology Co. (Guangzhou, China). Each treatment had three biological replicates.

RNA-seq data Filtering of Clean Reads, Denovo Assembly and Basic Annotation of Unigenes

Raw reads obtained from sequencing machines, including raw reads containing adapters or low-quality bases, affect subsequent assembly and analysis. Thus, to obtain high-quality clean reads, the reads were further filtered using Fastp software (version 0.18.0) [88]. The parameters were as follows: (1) reads containing adapters wer removed; (2) reads containing more than 10% of unknown nucleotides (N) were reomved; (3) low-quality reads containing more than 50% of low quality (Q-value ≤ 20) bases were removed. Transcriptome denovo assembly was conducted using the short reads assembly program, Trinity [89]. To annotate the unigenes, we used the BLASTx program (http://www.ncbi.nlm.nih.gov/BLAST/) with an E-value threshold of 1e-5 in the NCBI non-redundant protein (Nr) (http://www.ncbi.nlm.nih.gov), Swiss-Prot protein (http://www.expasy.ch/sprot), Kyoto Encyclopedia of Genes and Genomes (KEGG) (http://www.genome.jp/kegg), and COG/KOG databases (http://www.ncbi.nlm.nih.gov/COG). The protein with the highest sequence similarity to the given unigene was identified and the protein function annotation information of the unigene was obtained.

Differential expression and target genes analysis

The Omicsmart online data analysis platform (https://www.omicsmart.com/home.html#/) was used to calculate the differentially expressed genes (DEGs) between DT and DS genotypes under the control condition and 20% PEG-6000 treatment. Significant DEGs between the osmotic stress and control conditions were identified at |log2(foldchange) | > 2 and false discovery rate (FDR) adjusted $P < 0.001$. Subsequently, GO and KEGG pathway enrichment analysis was performed on the Omicsmart online data analysis platform (https://www.omicsmart.com/home.html#/) for differential basic genes in DT and DS under PEG-induced osmotic stress for 0, 3, and 24 h. Furthermore, a cluster heat map and trend analysis of the co-expressed genes were performed. Candidate genes with similar expression patterns were grouped together using the Omicsmart heatmap analysis tool (https://www.omicsmart.com/home.html#/). The clustering results were then divided into different trend blocks. Analysis of candidate genes trends using the Omicsmart trend analysis tool (https://www.omicsmart.com/home.html#/). Significant trend blocks were identified when $|\log2(\text{foldchange})| > 2$ and $P < 0.05$. The different profiles represent the numbers of the different trend blocks. Finally, pathway enrichment analysis was performed for candidate genes under osmotic stress.

Statistical analysis

Statistical analyses were performed using Microsoft Excel 2016. Analysis of physiological and phenotypic characterizations data was performed using IBM SPSS Statistics (version 26.0). Physiological and phenotypic characterizations values are shown as the mean ± standard deviation (SD) of biological replicates. Duncan's multiple range test was performed with a P-value < 0.05, considered significantly different. Origin 2021 was used for data visualization. The Omicsmart online data analysis platform (https://www.omicsmart.com/home.html#/) was used to visualize transcriptome sequencing data.

Conclusions

This study combined physiological and transcriptomic analyses to reveal differences in drought tolerance between two genotypes of *E. sibiricus*, DT and DS. The physiological and biochemical results confirmed that DT exhibited greater drought tolerance than DS. Transcriptome analysis identified multiple drought tolerance genes. By combining the physiological and biochemical results, we found that these genes may participate in several drought tolerance pathways in *E. sibiricus*, including ABA signaling pathway-induced stomatal closure, leaf cuticular wax deposition, ascorbic acid (ASA) metabolism, and reactive oxygen

species (ROS) scavenging. This study provides new insights into the mechanisms of drought tolerance in meso-xerophytic forage grass and provides a valuable basis for the genetic improvement of drought tolerance in forages and crops.

References

1. Moore, J. P., Vicre-Gibouin, M., Farrant, J. M. & Driouich, A. Adaptations of higher plant cell walls to water loss: drought vs desiccation. *Physiol Plant*. **134**, 237-245 (2008).
2. Zhang, H., Sun, X. & Dai, M. Improving crop drought resistance with plant growth regulators and rhizobacteria: Mechanisms, applications, and perspectives. *Plant Commun*. **3**, 100228 (2022).
3. Fang, Y. & Xiong, L. General mechanisms of drought response and their application in drought resistance improvement in plants. *Cell Mol Life Sci*. **72**, 673-689 (2015).
4. Razi, K. & Muneer, S. Drought stress-induced physiological mechanisms, signaling pathways and molecular response of chloroplasts in common vegetable crops. *Crit Rev Biotechnol*. **41**, 669-691 (2021).
5. Intergovernmental Panel on Climate, C. *Climate Change 2021 – The Physical Science Basis*. (2023).
6. Ault, T. R. On the essentials of drought in a changing climate. *Science*. **368**, 256-260 (2020).
7. Muller, L. M. & Bahn, M. Drought legacies and ecosystem responses to subsequent drought. *Glob Chang Biol*. **28**, 5086-5103 (2022).
8. Zhu, J. K. Abiotic Stress Signaling and Responses in Plants. *Cell*. **167**, 313-324 (2016).
9. Chaves, M. M., Maroco, J. P. & Pereira, J. S. Understanding plant responses to drought—from genes to the whole plant. *Funct Plant Biol*. **30**, 239-264 (2003).
10. Qi, J. *et al.* Reactive oxygen species signaling and stomatal movement in plant responses to drought stress and pathogen attack. *J Integr Plant Biol*. **60**, 805-826 (2018).
11. Geng, M. F. *et al.* Genome-wide investigation on transcriptional responses to drought stress in wild and cultivated rice. *Environ Exp Bot*. **189**, 104555 (2021).
12. Zhu, J. K. Salt and drought stress signal transduction in plants. *Annu Rev Plant Biol*. **53**, 247-273 (2002).
13. Mahajan, S. & Tuteja, N. Cold, salinity and drought stresses: an overview. *Arch Biochem Biophys*. **444**, 139-158 (2005).
14. Shinozaki, K. & Yamaguchi-Shinozaki, K. Gene networks involved in drought stress response and tolerance. *J Exp Bot*. **58**, 221-227 (2007).
15. Shao, H. B., Chu, L. Y., Jaleel, C. A. & Zhao, C. X. Water-deficit stress-induced anatomical changes in higher plants. *Cr Biol*. **331**, 215-225 (2008).
16. Pandey, V. & Shukla, A. Acclimation and Tolerance Strategies of Rice under Drought Stress. *Rice Sci*. **22**, 147-161 (2015).
17. Farooq, M., Wahid, A., Kobayashi, N., Fujita, D. & Basra, S. M. A. Plant drought stress: effects, mechanisms and management. *Agron Sustain Dev*. **29**, 185-212 (2009).
18. Zhang, H., Zhu, J., Gong, Z. & Zhu, J. K. Abiotic stress responses in plants. *Nat Rev Genet*. **23**, 104-119 (2022).
19. Verma, S., Negi, N. P., Pareek, S., Mudgal, G. & Kumar, D. Auxin response factors in plant adaptation to drought and salinity stress. *Physiol Plant*. **174**, e13714 (2022).
20. Reddy, A. R., Chaitanya, K. V. & Vivekanandan, M. Drought-induced responses of photosynthesis and antioxidant metabolism in higher plants. *J Plant Physiol*. **161**, 1189-1202 (2004).
21. Nezhadahmadi, A., Prodhan, Z. H. & Faruq, G. Drought tolerance in wheat. *Sci World J*. **2013**, 610721 (2013).
22. Waszczak, C., Carmody, M. & Kangasjärvi, J. Reactive Oxygen Species in Plant Signaling. *Annu Rev Plant Biol*. **69**, 209-236 (2018).
23. Cruz de Carvalho, M. H. Drought stress and reactive oxygen species: Production, scavenging and signaling. *Plant Signal Behav*. **3**, 156-165 (2008).
24. Desikan, R. *et al.* ABA, hydrogen peroxide and nitric oxide signalling in stomatal guard cells. *J Exp Bot*. **55**, 205-212 (2004).
25. Karpinska, B., Wingsle, G. & Karpinski, S. Antagonistic effects of hydrogen peroxide and glutathione on acclimation to excess excitation energy in *Arabidopsis*. *Iubmb Life*. **50**, 21-26 (2000).
26. Hsu, P. K., Dubeaux, G., Takahashi, Y. & Schroeder, J. I. Signaling mechanisms in abscisic acid-mediated stomatal closure. *Plant J*. **105**, 307-321 (2021).

27. Bi, H. *et al.* The impact of drought on wheat leaf cuticle properties. *BMC Plant Biol*. **17**, 1-13 (2017).
28. Tapia, G., Morales-Quintana, L., Parra, C., Berbel, A. & Alcorta, M. Study of nsLTPs in *Lotus japonicus* genome reveal a specific epidermal cell member (LjLTP10) regulated by drought stress in aerial organs with a putative role in cutin formation. *Plant Mol Biol*. **82**, 485-501 (2013).
29. Chen, G. *et al.* A functional cutin matrix is required for plant protection against water loss. *Plant Signal Behav*. **6**, 1297-1299 (2011).
30. Mohammadian, M. A., Watling, J. R. & Hill, R. S. The impact of epicuticular wax on gas-exchange and photoinhibition in *Leucadendron lanigerum* (Proteaceae). *Acta Oecol*. **31**, 93-101 (2007).
31. Grünhofer, P. *et al.* Changes in wax composition but not amount enhance cuticular transpiration. *Plant Cell Environ*. **47**, 91-105 (2023).
32. Joshi, R. *et al.* Transcription Factors and Plants Response to Drought Stress: Current Understanding and Future Directions. *Front Plant Sci*. **7**, 1029 (2016).
33. Zenda, T. *et al.* Key Maize Drought-Responsive Genes and Pathways Revealed by Comparative Transcriptome and Physiological Analyses of Contrasting Inbred Lines. *Int J Mol Sci*. **20**, 1268 (2019).
34. Wang, Y. *et al.* Transcriptomic and physiological responses of contrasting maize genotypes to drought stress. *Front Plant Sci*. **13**, 928897 (2022).
35. Wilkins, O., Bräutigam, K. & Campbell, M. M. Time of day shapes *Arabidopsis* drought transcriptomes. *Plant J*. **63**, 715-727 (2010).
36. Quan, R. *et al.* Overexpression of an ERF transcription factor *TSRF1* improves rice drought tolerance. *Plant Biotechnol J*. **8**, 476-488 (2010).
37. Cao, L. *et al.* Transcriptional regulatory networks in response to drought stress and rewatering in maize (*Zea mays* L.). *Mol Genet Genomics*. **296**, 1203-1219 (2021).
38. Sakuma, Y. *et al.* Functional analysis of an *Arabidopsis* transcription factor, DREB2A, involved in drought-responsive gene expression. *Plant Cell*. **18**, 1292-1309 (2006).
39. Fujita, Y. *et al.* AREB1 is a transcription activator of novel ABRE-dependent ABA signaling that enhances drought stress tolerance in *Arabidopsis*. *Plant Cell*. **17**, 3470-3488 (2005).
40. Liu, S. *et al.* Global Transcriptome and Weighted Gene Co-expression Network Analyses of Growth-Stage-Specific Drought Stress Responses in Maize. *Front Genet*. **12**, 645443 (2021).
41. Seki, M., Umezawa, T., Urano, K. & Shinozaki, K. Regulatory metabolic networks in drought stress responses. *Curr Opin Plant Biol*. **10**, 296-302 (2007).
42. Umezawa, T., Yoshida, R., Maruyama, K., Yamaguchi-Shinozaki, K. & Shinozaki, K. SRK2C, a SNF1-related protein kinase 2, improves drought tolerance by controlling stress-responsive gene expression in *Arabidopsis thaliana*. *P Natl Acad Sci Usa*. **101**, 17306-17311 (2004).
43. Ma, X., Chen, S., Zhang, X., Bai, S. & Zhang, C. Assessment of worldwide genetic diversity of Siberian wild rye (*Elymus sibiricus* L.) germplasm based on gliadin analysis. *Molecules*. **17**, 4424-4434 (2012).
44. Xie, W., Zhang, J., Zhao, X., Zhang, Z. & Wang, Y. Transcriptome profiling of Elymus sibiricus, an important forage grass in Qinghai-Tibet plateau, reveals novel insights into candidate genes that potentially connected to seed shattering. *BMC Plant Biol*. **17**, 1-15 (2017).
45. De, Y., Shi, F., Gao, F., Mu, H. & Yan, W. Siberian Wildrye (*Elymus sibiricus* L.) Abscisic Acid-Insensitive 5 Gene Is Involved in Abscisic Acid-Dependent Salt Response. *Plants*. **10**, 1351 (2021).
46 Zhang, Z. *et al.* High-Altitude Genetic Selection and Genome-Wide Association Analysis of Yield-Related Traits in *Elymus sibiricus* L. Using SLAF Sequencing. *Front Plant Sci*. **13**, 874409 (2022).
47. Yu, Q. *et al.* Comparative Metabolomic Studies of Siberian Wildrye (*Elymus sibiricus* L.): A New Look at the Mechanism of Plant Drought Resistance. *Int J Mol Sci*. **24**, 452 (2022).
48. Liu, X. *et al.* Endodermal apoplastic barriers are linked to osmotic tolerance in meso-xerophytic grass *Elymus sibiricus*. *Front Plant Sci*. **13**, 1007494 (2022).
49. Fricke, W. Water transport and energy. *Plant Cell Environ*. **40**, 977-994 (2016).
50. Martinez-Vilalta, J. & Garcia-Forner, N. Water potential regulation, stomatal behaviour and hydraulic transport under drought: deconstructing the iso/anisohydric concept. *Plant Cell Environ*. **40**, 962-976 (2017).

51. Franks, P. J. Higher rates of leaf gas exchange are associated with higher leaf hydrodynamic pressure gradients. *Plant Cell Environ*. **29**, 584-592 (2006).
52. Ampomah-Dwamena, C. *et al.* A kiwifruit (*Actinidia deliciosa*) R2R3-MYB transcription factor modulates chlorophyll and carotenoid accumulation. *New Phytol*. **221**, 309-325 (2019).
53. Rouhi, V., Samson, R., Lemeur, R. & Damme, P. V. Photosynthetic gas exchange characteristics in three different almond species during drought stress and subsequent recovery. *Environ Exp Bot*. **59**, 117-129 (2007).
54. Li, J. *et al.* Defense-related transcription factors WRKY70 and WRKY54 modulate osmotic stress tolerance by regulating stomatal aperture in *Arabidopsis*. *New Phytol*. **200**, 457-472 (2013).
55. Liu, H. *et al.* Signaling Transduction of ABA, ROS, and Ca^{2+} in Plant Stomatal Closure in Response to Drought. *Int J Mol Sci*. **23**, 14824 (2022).
56. Lim, C., Baek, W., Jung, J., Kim, J.-H. & Lee, S. Function of ABA in Stomatal Defense against Biotic and Drought Stresses. *Int J Mol Sci*. **16**, 15251-15270 (2015).
57. Takahashi, F., Kuromori, T., Sato, H. & Shinozaki, K. Regulatory Gene Networks in Drought Stress Responses and Resistance in Plants. *Survival Strategies in Extreme Cold and Desiccation*. 189-214 (2018).
58. Zhang, Y. *et al.* Wheat ABA Receptor TaPYL5 Constitutes a Signaling Module with Its Downstream Partners TaPP2C53/TaSnRK2.1/TaABI1 to Modulate Plant Drought Response. *Int J Mol Sci*. **24**, 7969 (2023).
59. Lim, C. W., Yang, S. H., Shin, K. H., Lee, S. C. & Kim, S. H. The AtLRK10L1.2, *Arabidopsis* ortholog of wheat LRK10, is involved in ABA-mediated signaling and drought resistance. *Plant Cell Rep*. **34**, 447-455 (2015).
60. Huang, S. *et al.* CBL4-CIPK5 pathway confers salt but not drought and chilling tolerance by regulating ion homeostasis. *Environ Exp Bot*. **179**, 104230 (2020).
61. Kunst, L. & Samuels, A. L. Biosynthesis and secretion of plant cuticular wax. *Prog Lipid Res*. **42**, 51-80 (2003).
62. Shellakkutti, N. *et al.* Cuticular transpiration is not affected by enhanced wax and cutin amounts in response to osmotic stress in barley. *Physiol Plantarum*. **174**, e13735 (2022).
63. Samuels, L., Kunst, L. & Jetter, R. Sealing Plant Surfaces: Cuticular Wax Formation by Epidermal Cells. *Annu Rev Plant Biol*. **59**, 683-707 (2008).
64. He, J. *et al. ECERIFERUM1-6A* is required for the synthesis of cuticular wax alkanes and promotes drought tolerance in wheat. *Plant Physiol*. **190**, 1640-1657 (2022).
65. Lewandowska, M., Keyl, A. & Feussner, I. Wax biosynthesis in response to danger: its regulation upon abiotic and biotic stress. *New Phytol*. **227**, 698-713 (2020).
66. Sanjari, S. *et al.* Molecular, chemical, and physiological analyses of sorghum leaf wax under post-flowering drought stress. *Plant Physiol Bioch*. **159**, 383-391 (2021).
67. Dimopoulos, N. *et al.* Drought stress modulates cuticular wax composition of the grape berry. *J Exp Bot*. **71**, 3126-3141 (2020).
68. Li, T. *et al.* TaCER1-1A is involved in cuticular wax alkane biosynthesis in hexaploid wheat and responds to plant abiotic stresses. *Plant Cell Environ*. **42**, 3077-3091 (2019).
69. Wang, D., Ni, Y., Liao, L., Xiao, Y. & Guo, Y. Poa pratensis *ECERIFERUM1 (PpCER1)* is involved in wax alkane biosynthesis and plant drought tolerance. *Plant Physiol Bioch*. **159**, 312-321 (2021).
70. Wu, H. *et al.* Tomato SlCER1–1 catalyzes the synthesis of wax alkanes, increasing drought tolerance and fruit storability. *Hortic Res-England*. **9**, uhac004 (2022).
71. Wen, H. *et al.* Analysis of Wheat Wax Regulation Mechanism by Liposome and Transcriptome. *Front Genet*. **12**, 757920 (2021).
72. Harb, A. *et al.* The Effect of Drought on Transcriptome and Hormonal Profiles in Barley Genotypes With Contrasting Drought Tolerance. *Front Plant Sci*. **11**, 618491 (2020).
73. Wu, H. *et al.* Expression Analysis and Functional Characterization of *CER1* Family Genes Involved in Very-Long-Chain Alkanes Biosynthesis in *Brachypodium distachyon*. *Front Plant Sci*. **10**, 1389 (2019).

74. Pascal, S. *et al. Arabidopsis* CER1-LIKE1 Functions in a Cuticular Very-Long-Chain Alkane-Forming Complex. *Plant Physiol*. **179**, 415-432 (2019).
75. Mittler, R., Zandalinas, S. I., Fichman, Y. & Van Breusegem, F. Reactive oxygen species signalling in plant stress responses. *Nat Rev Mol Cell Biol*. **23**, 663-679 (2022).
76. Mittler, R. ROS Are Good. *Trends Plant Sci*. **22**, 11-19 (2017).
77. Apel, K. & Hirt, H. REACTIVE OXYGEN SPECIES: Metabolism, Oxidative Stress, and Signal Transduction. *Annu Rev Plant Biol*. **55**, 373-399 (2004).
78. Moustafa-Farag, M. *et al.* Role of Melatonin in Plant Tolerance to Soil Stressors: Salinity, pH and Heavy Metals. *Molecules*. **25**, 5359 (2020).
79. Hong, X. *et al.* Ascorbate peroxidase 1 allows monitoring of cytosolic accumulation of effector-triggered reactive oxygen species using a luminol-based assay. *Plant Physiol*. **191**, 1416-1434 (2023).
80. Amancio, S. *et al.* Photosynthetic and ascorbate-glutathione metabolism in the flag leaves as compared to spikes under drought stress of winter wheat (*Triticum aestivum* L.). *Plos One*. **13**, e0194625 (2018).
81. Han, S. H., Park, Y. J. & Park, C. M. Light Primes the Thermally Induced Detoxification of Reactive Oxygen Species During Development of Thermotolerance in *Arabidopsis*. *Plant Cell Physiol*. **60**, 230-241 (2019).
82. Li, H. B. *et al.* A cotton ascorbate peroxidase is involved in hydrogen peroxide homeostasis during fibre cell development. *New Phytol*. **175**, 462-471 (2007).
83. Sun, Y. *et al.* WRKY33-PIF4 loop is required for the regulation of H_2O_2 homeostasis. *Biochem Bioph Res Co*. **527**, 922-928 (2020).
84. Pal, P. *et al.* Genome-wide transcriptional profiling and physiological investigation elucidating the molecular mechanism of multiple abiotic stress response in *Stevia rebaudiana* Bertoni. *Sci Rep-Uk*. **13**, 19853 (2023).
85. Zhao, F., Wu, Y., Ma, S., Lei, X. & Liao, W. Increased water use efficiency in China and its drivers during 2000–2016. 1-17 (2022).
86. Song, X., Zhou, G., He, Q. & Zhou, H. Stomatal limitations to photosynthesis and their critical Water conditions in different growth stages of maize under water stress. *Agr Water Manage*. **241**, 106330 (2020).
87. Jenkin, S. & Molina, I. Isolation and Compositional Analysis of Plant Cuticle Lipid Polyester Monomers. *J Vis Exp*. e53386 (2015).
88. Chen, S., Zhou, Y., Chen, Y. & Gu, J. fastp: an ultra-fast all-in-one FASTQ preprocessor. *Bioinformatics*. **34**, i884-i890 (2018).
89. Grabherr, M. G. *et al.* Full-length transcriptome assembly from RNA-Seq data without a reference genome. *Nat Biotechnol*. **29**, 644-652 (2011).

Acknowledgments

We are very grateful to Sichuan Zoige Alpine Wetland Ecosystem National Observation and Research Station and College of Grassland Resources, Institute of Qinghai-Tibetan Plateau, Southwest Minzu University for providing us with experimental equipment and venue. Thanks to all authors for their hard work on this manuscript. We are grateful thank Guangzhou Gene Denovo Biotechnology Co., Ltd for assisting in sequencing and bioinformatics analysis. Thank you to Editage for polishing our manuscript!

Author contributions statement

Conceptualization, Y.A. and Pe.W.; methodology, X.L., Pi.W. and Pe.W.; software, Y.A. and Y.Z.; investigation, X.L., Pi.W., Y.Z. and Y.A.; resources, Q.Z., Y.Ch. and Pe.W.; data curation, Y.A., Y.Z. and Pe.W.; writing—original draft preparation, Y.A. and Pe.W.; writing—review and editing, Y.A., Q.W., Y.C., P.K., Z.W. and Pe.W. All authors have read and agreed to the published version of the manuscript.

Competing interests

Te authors declare no competing interests.

Supplementary Files

This is a list of supplementary files associated with this preprint. Click to download.

- Supplementary.zip